



Transcription factor CgPOU3F4-like regulates expression of pheomelanin synthesis related gene *CgB-aat1* in the Pacific oyster (*Crassostrea gigas*)

Zhuanzhuan Li^a, Chengxun Xu^a, Hong Yu^a, Lingfeng Kong^a, Shikai Liu^a, Qi Li^{a,b,*}

^a Key Laboratory of Mariculture, Ministry of Education, Ocean University of China, Qingdao 266003, China

^b Laboratory for Marine Fisheries Science and Food Production Processes, Qingdao National Laboratory for Marine Science and Technology, Qingdao 266237, China

ARTICLE INFO

Edited by Dr. Marco Barucca

Keywords:

CgPOU3F4-like

CgB-aat1

Regulation of gene expression

RNA interference

Crassostrea gigas

ABSTRACT

Previous study has found that b (0, +) -type amino acid transporter 1 (*CgB-aat1*) plays an essential role on mantle pigmentation in the Pacific oyster *Crassostrea gigas*. However, the molecular regulation of *CgB-aat1* gene expression remains unclear. Herein, three POU domain family members, *CgPOU2F1*, *CgPOU3F4-like* and *CgPOU4F3-X1* were characterized and they all had POU and HOX domains, respectively, which were important in transcriptional regulation. *CgPOU3F4-like* gene expression was the highest in mantle edge. Subsequently, the dual-luciferase reporter result showed that the core regulatory region of *CgB-aat1* gene was from -632 to -350 bp of promoter. In transient co-transfection assays, the strongest activity was activated only by *CgPOU3F4-like*, suggesting *CgPOU3F4-like* was a valid transcriptional activator of *CgB-aat1* gene promoter. And the structural integrity of *CgPOU3F4-like* was essential for its activation function. In addition, site directed mutagenesis assay was applied to detect three key binding sites between *CgPOU3F4-like* and core region of *CgB-aat1* gene promoter, and this interaction was verified by ChIP test. Furthermore, *CgPOU3F4-like* knockdown by RNA interference led to obvious decreases in *CgB-aat1* and cystathionine beta-synthase (*CgCbs*) expressions at both mRNA and protein levels. Collectively, these results indicate that *CgPOU3F4-like* positively regulate *CgB-aat1* gene expression and it may be a critical upstream transcriptional regulation factor in pheomelanin synthesis in *C. gigas*.

1. Introduction

Molluscan shellfish have traditionally been a major product of world aquaculture, their shells with diverse colors and patterns have attracted numerous collectors and also influenced consumer preference. The diversity of shell color greatly enriches the multiformity of biological color. So far, shell color as an economic trait has been widely concerned by breeders, several shell colors as targeted trait have been successfully developed in bivalves, like oysters (Evans et al., 2009; Vu et al., 2020), scallops (Wang et al., 2017) and clams (Liang et al., 2019). However, the knowledge of pigment components, formation process and molecular basis of shell color are still scarce, which limit the further application of shell color trait. Therefore, it is important to study the formation mechanism of shell color not only for the understanding of the evolution

law of body color, but also for the cultivation of better varieties of shellfish.

Shell color formation is closely linked to the creation, deposition, and transport of pigments, among which melanin has been the major research object so far (Williams, 2017). At present, two different types of melanin (eumelanin and pheomelanin) have been identified in shell of Gastropod *Cepaea nemoralis* using high-performance liquid chromatography (Affenzeller et al., 2019). Related genes, such as tyrosinase (*Tyr*), tyrosinase-related protein (*Tyrp*), microphthalmia-associated transcription factor (*Mitf*) and paired box 3/7 (*Pax3/7*) have been found to regulate melanin deposition in mollusks through omics analysis or gene function verification (Lemer et al., 2015; Li et al., 2021, 2022b; Nie et al., 2020; Palumbo, 2003; Saenko and Schilthuizen, 2021; Yu et al., 2018a,b; Zhang et al., 2018). Additionally, solute carrier family 7

Abbreviations: B-aat1, b (0, +) -type amino acid transporter 1; Cbs, cystathionine beta-synthase; ChIP, chromatin immunoprecipitation; e1f1 α , α subunit of elongation factor 1; Elisa, enzyme-linked immunosorbent assay; GAPDH, glyceraldehyde-3-phosphate dehydrogenase; Mitf, microphthalmia-associated transcription factor; Pax3/7, paired box 3/7; POU2F1, POU domain, class 2, transcription factor 1; POU3F4-like, POU domain, class 3, transcription factor 4-like; POU4F3-X1, POU domain, class 4, transcription factor 3 isoform X1; qPCR, real-time quantitative polymerase chain reaction; RNAi, RNA interference; Slc7a11, solute carrier family 7 member 11 (xCT); TYR, tyrosinase; TYRP, tyrosinase-related protein; WB, western blot.

* Corresponding author at: Key Laboratory of Mariculture, Ministry of Education, Ocean University of China, Qingdao, China.

E-mail address: qili66@ouc.edu.cn (Q. Li).

<https://doi.org/10.1016/j.gene.2023.147258>

Received 12 December 2022; Received in revised form 24 January 2023; Accepted 3 February 2023

Available online 6 February 2023

0378-1119/© 2023 Elsevier B.V. All rights reserved.

member 11 (xCT) (*slc7a11*) acts as a vector to transport extracellular cystine, which is required for the production of pheomelanin. To date, a primary understanding of the mechanisms associated with melanin pigmentation has been obtained through extensive study of the type of melanin in shell and functional analysis of melanin synthesis related genes. However, very little is known about the intracellular regulation of melanin pigmentation related genes in mollusks.

The transcription factor POU family participates in regulating transcription of genes involved in various physiology processes (Besch and Berking, 2014; Candiani et al., 2002; Wang et al., 2012). Structurally, the POU family shares a common DNA binding domain, the POU domain, which consists of an N-terminal POU-specific domain (POU_S), a C-terminal homeodomain (POU_H, HOX) and a variable linker connecting the two (Ryan and Rosenfeld, 1997). POU family is grouped into six major classes based on the sequence alignment and diverse biological function (Gold et al., 2014). POU2F1, also known as OCT1, is one of the POU family and ubiquitously expressed in both embryonic and adult tissues (Zhang et al., 2013). Recent studies of POU2F1 have focused on its effects on growth regulation and disease development (Sreenivasan and Viljoen, 2013). Furthermore, POU2F1 was also found to modulate *Slc7a11* gene expression by binding to the promoter regions and played a regulatory role in Rex rabbit pigmentation (Chen et al., 2019; Yang et al., 2020). The other member, POU3F4, also known as brn-4, are mainly brain-specific with neuronal development related function (Andersen and Rosenfeld, 2001). Similar to the POU3F4 proteins, the POU4F3 also mainly act in regulating the development of sensory nervous system (Erkman et al., 1996). However, there was no evidence that POU3F4 or POU4F3 was involved in pigmentation regulation. Compared with the studies of POU factors in vertebrates, little information is available on POU family genes function in mollusks (Lozano et al., 2014; Min et al., 2022a). It was reported that POU family genes acted on the development of sensory cell and nervous system in gastropod (O'Brien and Degnan, 2000, 2002; Wollesen et al., 2014) as well as regulated the expression of matrix protein genes and shell pigmentation genes in oysters (Gao et al., 2016; Min et al., 2022b). Nevertheless, the regulatory role of POU transcription factors in shell pigmentation is still severely scarce in mollusks.

The Pacific oyster, *Crassostrea gigas*, is one of the most economically important marine bivalve species. Previous study suggested that *CgB-aat1* (named *Slc7a11* in vertebrate) played an important role in mantle pigmentation in *C. gigas* (Li et al., 2022c). Given that POU transcription factors are usually involved in various biological processes, if they participate in pigmentation in mollusks is still unclear. Hence, it is necessary to clarify the transcriptional regulation of POU family members on *CgB-aat1* gene and the function in pigmentation. In the present study, the molecular characteristics and expression patterns of *POU2F1*, *POU3F4-like* and *POU4F3-X1* in *C. gigas* were analyzed. Furthermore, the regulatory role of transcription factors in *CgB-aat1* gene expression was also studied. These data enrich the knowledge of regulation mechanisms of *CgB-aat1* gene expression and provide valuable information on shell coloration, which is useful for selective breeding of different shell coloration lines of *C. gigas*.

2. Materials and methods

2.1. Sample collection

The Pacific oysters were collected from the Rongcheng, Shandong Province, China, and maintained in tanks prior to experimentation. During the acclimation, the oysters were cultured in aerated seawater at 24 ± 1 °C and were fed with *Chlorella vulgaris* three times daily prior to renew seawater twice a day. Seven days later, a total of eighteen oysters (shell length: 24.02 ± 8.09 cm; shell height: 36.55 ± 9.08 cm) were randomly chosen. Six tissues including mantle edge, central mantle, gill, labial palp, adductor muscle and digestive gland were sampled for RNA isolation and every three in same tissues were mixed as one RNA sample.

The Pacific oyster is neither an endangered nor protected species. All experiments in our study were conducted according to national and institutional guidelines.

2.2. Sequence analysis

The amino acid (aa) sequences of POU domain, class 2, transcription factor 1 (POU2F1) and POU domain, class 3, transcription factor 4-like (POU3F4-like) and POU domain, class 4, transcription factor 3 isoform X1 (POU4F3-X1) in *C. gigas* (*CgPOU2F1*, XP_034303537.1; *CgPOU3F4-like*, XP_034335340.1; *CgPOU4F3-X1*, XP_011456596.1) were retrieved from NCBI database. The sequence analysis of *CgPOU2F1* was implemented as described previously (Min et al., 2022a). Here, the sequences of *CgPOU3F4-like* and *CgPOU4F3-X1* were characterized. The POU2F1, POU3F4 and POU4F3 sequences from other species were obtained from NCBI and accession numbers were listed in Table S2. The function structure domain of amino acid was predicted using SMART (<http://smart.embl-heidelberg.de/>). Multiple sequence alignments of amino acids were proceeded using DNAMAN 8.0. A phylogenetic tree was constructed by the maximum-likelihood algorithm with Jones-Taylor-Thornton (JTT) + Gamma Distributed (G) model using the MEGA X with bootstrap method and 1000 replications.

2.3. Gene expression analysis by real-time quantitative PCR

Trizol (Invitrogen, USA) was used to extract total RNA based on provided directions, a PrimeScript™ RT reagent Kit with gDNA Eraser (Takara, China) was used to prepare cDNA. The qPCR primer pairs for target genes and reference genes α subunit of elongation factor 1 (*ef1 α*) (Du et al., 2013) were listed in Table 1. QuantiNova™ SYBR® Green PCR (QIAGEN, Germany) system was used for qPCR following the instruction manual. Briefly, the following were mixed in a PCR: 5 μ L 2 \times SYBR Green PCR Master Mix, 1 μ L cDNA template, 1 μ L each 10 mM primer and 2 μ L RNase-free water. The LightCycler 480 (Roche, Switzerland) real-time thermal cycler was set to the following parameters: 95 °C for 2 min, followed by 40 cycles of 95 °C for 5 s and 60 °C for 10 s. Primers were tested and selected for efficiency and specificity (Table S1). All qPCR reactions were executed in triplicate for each cDNA sample. Gene expression was measured using $2^{-\Delta\Delta CT}$ method (Livak and Schmittgen, 2001) and all data was shown as means \pm standard error (SE) ($n = 6$). Statistical analysis was performed using one-way analysis of variance (ANOVA) method by SPSS 17.0 and significant difference was considered at $P < 0.05$.

2.4. Plasmid construction

The mRNA sequences of *CgPOU2F1* (XM_034447646.1), *CgPOU3F4-like* (XM_034479449.1) and *CgPOU4F3-X1* (XM_011458294.3) were retrieved from NCBI database. The whole CDS sequence of *CgPOU2F1*, *CgPOU3F4-like* and *CgPOU4F3-X1* were generated by PCR based on the primers (Table 1) using 2 \times Taq Plus Master Mix (Vazyme, China). Subsequently, the coding regions of *CgPOU2F1*, *CgPOU3F4-like* and *CgPOU4F3-X1* were sub-cloned into expression vectors pcDNA3.1(+) (Promega, USA) using ClonExpress® Ultra One Step Cloning Kit (Vazyme, China). Additionally, C-terminal deletion constructs POU3F4-like-1, POU3F4-like -2 and POU3F4-like -3 of POU3F4-like were generated in pcDNA3.1(+) plasmid, respectively.

CgB-aat1 gene sequence was obtained from the genome sequence in NCBI database (Gene ID: 105339508). The promoter regions of *CgB-aat1* were designed from upstream of 3 kb in *CgB-aat1* gene sequence. A 3 kb fragment of *CgB-aat1* was amplified using genomic DNA template of *C. gigas* and sub-cloned into pGL3-Basic vector (Promega, USA). In addition, five truncations from *CgB-aat1* gene promoter, B-aat1-1 (-1800 to + 344), B-aat1-2 (-1500 to + 344), B-aat1-3 (-1280 to + 344), B-aat1-4 (-632 to + 344) and B-aat1-5 (-350 to + 344) were also generated in pGL3-basic vector, respectively. The site-directed mutagenesis

Table 1
Sequences information of specific primers.

Gene name	Primer	Sequence (5'-3')	Application
EGFP, Enhanced green fluence protein	EGFP-F	ACGTAAACGGCCACAAGTTC	dsRNA synthesis in RNAi
	EGFP-R	TGTTCTGCTGGTAGTGGTCG	
POU2F1, POU domain, class 2, transcription factor 1	POU2F1-F	CTCTTCGGTGGGACCAATC	qPCR
	POU2F1-R	GCTTTTTGCAGGGTAAGCCC	
POU3F4-like, POU domain, class 3, transcription factor 4-like	POU2F1-F	ctagcgtttaaacttaagcttGTCTCTGCTTCTCAACCAATCAA	Plasmid Construction
	POU2F1-R	gccctctagactcgagcgccgctTTTAAATCTCACAAAATATAAATCTGATT	
	POU3F4-like-F	CGGGTTTGGTCTGCAACAG	qPCR
	POU3F4-like-R	GTCTGTGAGGAGGACTGC	
	POU3F4-like -F	ctagcgtttaaacttaagcttATGATGACCATGGCTACTAGCGC	Plasmid Construction
	POU3F4-like-R	gccctctagactcgagcgccgctCAGTGCCTCGGGGAATG	
	POU3F4-like -T1-R	gccctctagactcgagcgccgctCATCCGTTTCTCCTTTTGTCTCC	qPCR
	POU3F4-like-T2-R	gccctctagactcgagcgccgctACTTGTGGTTGAGCCAGTGGTG	
	POU3F4-like -T3-R	gccctctagactcgagcgccgctCTGGTCCCTCATGGCG	qPCR
	POU3F4-like-Myc-F	ggtcgaccgagatctctcgagATGATGACCATGGCTACTAGCGC	
POU4F3-X1, POU domain, class 4, transcription factor 3-X1	POU3F4-like-Myc-R	cagcttctgctcgggtaccTCAGTGCCTCGGGGAATG	PCR in ChIP
	POU3F4-like-ChIP-F1	AAATGTTTGTAGCAGGGACG	
	POU3F4-like-ChIP-R1	ACGCACGGTATCGACAAAAT	qPCR
	POU3F4-like-ChIP-F2	GAACGTCAAAAACATTCAACCAGC	
	POU3F4-like-ChIP-R2	ATACGTCCTGCTAACAAACAT	PCR in RNAi
	POU3F4-like-F	ATTCTTGAACACGGGGATG	
	POU3F4-like-R	CCTCTCGAGCCATTTTGTGA	qPCR in RNAi
	POU3F4-like-RNAi-F	TGGCCCGGATTTTGTCTAT	
	POU3F4-like-RNAi-R	GACTCGCACTCGGAACCTTA	qPCR
	POU4F3-X1-F	TTCAGGCTTGGCTCGAAGAG	
B-aat1, b (0, +)-type amino acid transporter 1	POU4F3-X1-R	CGCGAAATACGCTTCCAGTG	Plasmid Construction
	POU4F3-X1 -F	ctagcgtttaaacttaagcttAAGAGAATCTATCGAAACGAAGGC	
	POU4F3-X1-R	gccctctagactcgagcgccgctAATGAGACAGGTAAAATAAACCCACCA	Plasmid Construction
	POU4F3-X1-R	gcgtgtagccccggctcgagATCTTCATAAATCCGAATGAAAAAGTA	
	B-aat1-T1-R	cagtaccggaatccaagcttTTGTCTATAATTTCCACAGCAGACG	PCR for mutated B-aat1 promoter sequence
	B-aat1-T2-F	gcgtgtagccccggctcgagGTAATCTTCATGCTTTATGTAGAAAGTTT	
	B-aat1-T3-F	gcgtgtagccccggctcgagGATGGGATTTTCTTTGCTAAAATATAGG	qPCR
	B-aat1-T4-F	gcgtgtagccccggctcgagGGGGTGGCGGCTAATATTACT	
	B-aat1-T5-F	gcgtgtagccccggctcgagAATATATTTAAATAAAGAAAACCTCGAAGCA	qPCR
	B-aat1-Mut1-F	GACAacgtacatATACATGTACATAGTTTCTCCATAAAAAT	
B-aat1-Mut1-R	GTATAatgactgtGTCTCTTTACTAGGGTTGTAGTCTTTGA	qPCR	
B-aat1-Mut2-F	CGTAtgcagtcaAGTTTCTCCATAAAAATGTTTGTAGC		
B-aat1-Mut2-R	AACtTgcactgcaTACGTATGCATACATCTCTTACTAGGG	qPCR	
B-aat1-Mut3-F	TGCataacctgcGGCATTTTTTCCCTTCAGATGATT		
B-aat1-Mut3-R	AATGCTGcaggtatAGAGACACATATAACAGTTAGTATATACGTCCTC	qPCR	
B-aat1-F	GCTCTGGAATGGGAGAAGTAG		
B-aat1-R	CCCGTTAGCAGCACCAATG	qPCR	
Cbs, cystathionine beta-synthase	Cbs-F		TGGAGAAATCCCAGATGCC
Efl α , α subunit of elongation factor 1	Cbs-R	CGACCACAACCATGTCCACT	qPCR
	Efl α -F	ACGAATCTCTCCAGAGGCT	
	Efl α -R	GAAGTCTTGGCGCCCTTTG	

Note: The lowercase nucleotide sequences represent homologous arms sequence in Plasmid Construction experiments. The lowercase nucleotide sequences represent mutated site sequences in mutation experiments.

constructs were produced following the manufacturer's instructions of Mut Express Multi Fast Mutagenesis kit V2 (Vazyme, China). All the constructed plasmids were verified by sequencing analysis and the primer sequences used here were provided in Table 1.

2.5. Cell culture, transfection and dual luciferase assay

HEK-293 T cells were cultivated in Dulbecco's modified Eagle's medium (Solarbio, China) supplemented with 10% fetal bovine serum (Hyclone, USA) and 1% 1 X penicillin-streptomycin antibiotics solution (Hyclone, USA) at 37 °C with 5% CO₂. Cells were transfected using lipofectamine 3000 (Invitrogen, CA, USA) in accordance with the manufacturer's instructions when cells were grown at confluence of

70% – 90% in 24-well plates (Corning, USA). To normalize the transfection efficiency, pRL-TK (Promega, USA) was co-transfected as an internal control. In the study of basic activity of promoter, 500 ng B-aat1-1- pGL3, B-aat1-2- pGL3, B-aat1-3- pGL3, B-aat1-4- pGL3 and B-aat1-5- pGL3 or pGL3 and 5 ng pRL-TK were used for adding in each well of a 24-well plate. In the study of regulation of transcription factors, 250 ng recombinant pcDNA3.1 expression vector, 250 ng recombinant pGL3-Basic vector and 5 ng pRL-TK plasmid were used for adding in each well of a 24-well plate. After 48 h of transfection, dual luciferase assay was performed using Dual-Luciferase® Reporter Assay System (Promega, USA) according to the manufacturer's protocol. Briefly, following removing the medium, cells were washed with 1 × PBS (Solarbio, China) quickly at room temperature and were lysed using luciferase lysis buffer

(Promega, USA). Firefly and Renilla luciferase activities were measured using Multimode Microplate Reader (Synergy H1, BioTek, USA). The significance was analyzed by one-way ANOVA using SPSS 17.0 software.

2.6. Chromatin immunoprecipitation

Plasmid construction, cell culture and transfection were performed as described above, and coding region of *CgPOU3F4-like* was sub-cloned into the expression vectors pCMV-Myc-C (MiaoLing, China) for Chromatin immunoprecipitation (ChIP) experiment. ChIP experiment was applied using ChIP Assay Kit (Beyotime, China) following the manufacturer's instructions. The anti-Myc tag antibody (Boster, China) was used to bind to the object in this study. Samples without antibody were negative control and without cells were used as blank control. Finally, amplification was performed using two pair primers, respectively (Table 1). The product of PCR was examined on agarose gel electrophoresis.

2.7. Synthesis and injection of dsRNA

The 537 bp fragment of *CgPOU3F4-like* and 400 bp of enhanced green fluorescent protein (EGFP) were amplified using primers listed in Table 1. The purified PCR product was sub-cloned to *pEASY-T1* vector (TRANS, China) and sequenced to validate sense and antisense recombinant plasmid. The linearized plasmid was transcribed *in vitro* to synthesize dsRNA using a T7 RiboMAX™ Express RNAi System (Promega, USA) following the manufacturer's directions. The synthesized dsRNA was dissolved in nuclease-free water, and the final concentration of dsRNA was adjusted to 1 µg/µL.

After adaptation, twenty healthy oysters were randomly selected in each group and injected with 40 µL dsRNA (a total of 40 µg in per oyster) into adductor muscle in RNA interference (RNAi) group, the same dosage dsEGFP was injected in negative control, while as blank control, twenty oysters were injected nuclease-free water at the same dosage. A total of three injections were carried out on day 1, 4 and 7. Mantle tissue of six oysters were collected separately from each group at 24 h after the last injection and cryopreserved immediately. Preparation of the cDNA templates and determination of relative gene expression levels were performed as described above. *CgPOU3F4-like* expression was used to analysis gene silencing efficiency. Transcriptional and translational levels of *CgB-aat1* and *CgCbs* genes were also tested for determination of regulating effect of *CgPOU3F4-like*.

2.8. Western blot

Mantle tissues of six oysters were collected from three groups in RNAi experiment, respectively, and then the whole protein was extracted from each sample. In detail, mantle was homogenized in 1 × PBS buffer and centrifuged at 13,000 g for 15 min, then the supernatants were collected to measure the protein concentration using BCA Protein Assay Kit (Beyotime, China). Proteins of each sample (20 µg) were separated on 12.5 % (v/v) SDS-polyacrylamide gels and transferred to PVDF membranes (Beyotime, China). The membrane was blocked with 5% skimmed milk for 2 h at room temperature. Next, membrane was incubated with POU3F4 (Abclonal, China)/ *CgB-aat1*/ *CgCbs* polyclonal antibody (diluted 1: 1000 in Blocking Buffer) prepared by Li et al. (2022c) at 4 °C overnight and then incubated with HRP-conjugated goat anti-rabbit IgG (diluted 1: 1000 in Blocking Buffer, Beyotime, China) at 37 °C for 2 h. The proteins were detected using the enhanced ECL chemiluminescence detection reagents (Vazyme, China) and visualized with a GE ImageQuant LAS4000 mini system.

2.9. Enzyme-linked immunosorbent assay

Phemelanin content in mantle of six oysters from three groups in

RNAi experiment were measured respectively using enzyme-linked immunosorbent assay (Yanzunbio, China) according to the instructions. Briefly, 0.2 g mantle tissue were homogenized in 1 × PBS and centrifuged at 3000 g for 15 min to obtain the supernatant. Then, 50 µL of supernatant were incubated in Elisa plate at 37 °C for 30 min and then incubated with HRP-conjugated reagent at 37 °C for 30 min. After chromogenic reaction at 37 °C in dark for 10 min, absorbance of mixture was measured at 450 nm using Multimode Microplate Reader (Synergy H1, BioTek, USA).

3. Results

3.1. Sequence and phylogenetic analysis of *CgPOU2F1*, *CgPOU3F4-like* and *CgPOU4F3-X1*

Functional domain analysis showed that *CgPOU2F1*, *CgPOU3F4-like* and *CgPOU4F3-X1* all had a POU (POUs) domain and a HOX domain (Fig. 1A). Alignment of partial aa sequences from nigh species revealed high conservation of POU and HOX domains in three POU family members, with only a few different residues (Fig. 1A). The phylogenetic analysis presented that these three POU proteins belonged to different POU classes. Each of the three proteins clustered with proteins of the same class from other species, and were clearly separated from each other on different branches (Fig. 1B). Furthermore, *CgPOU2F1*, *CgPOU3F4-like* and *CgPOU4F3-X1* clustered with their homologs in *C. virginica*, *Pinctada fucata* and *Mytilus coruscus*, all these species belong to the group of Bivalves (Fig. 1B). All the molluscan POU2F1/POU3F4 (except for *OsPOU3F4*) were clustered together to form an invertebrate clade, separated from the vertebrate clade. The POU4F3 of *C. gigas* clustered with those of bivalves and then with that of *Octopus sinensis*, and finally clustered with vertebrates.

3.2. Tissue distributions of *CgPOU2F1*, *CgPOU3F4-like* and *CgPOU4F3-X1*

The amounts of *CgPOU2F1*, *CgPOU3F4-like* and *CgPOU4F3-X1* mRNAs in six tissues were determined by qPCR. Although *CgPOU2F1*, *CgPOU3F4-like* and *CgPOU4F3-X1* mRNAs were ubiquitously expressed in the analyzed six tissues, their expression patterns differed (Fig. 2). The expression of *CgPOU2F1* mRNA was highest in digestive gland, followed by labial lap, gill, adductor muscle and mantle edge, the lowest was in central mantle. *CgPOU3F4-like* mRNA was mainly present in mantle edge, gill, labial lap and adductor muscle. While *CgPOU4F3-X1* was mainly expressed in gill, with lower expression in adductor muscle (Fig. 2).

3.3. *CgPOU3F4-like* activated the promoter activity of *CgB-aat1* gene

Twelve binding sites in promoter region of *CgB-aat1* gene were predicted (Fig. 3A). The dual-luciferase reporter assay showed that transcriptional activity was significantly decreased with the deletion of *CgB-aat1* 5' flanking sequence (Fig. 3A). The significant decrease in the promoter activity was observed after deletion of -632 - -350 fragment, suggesting this segment might be the core promoter regulatory region of *CgB-aat1*. The strongest luciferase activity was detected when *CgPOU3F4-like* and *CgB-aat1* co-transfection, however, *CgPOU2F1* and *CgPOU4F3-X1* had a limited effect on promoter activity of *CgB-aat1*, which revealed that *CgPOU3F4-like* was a valid transcriptional activator of *CgB-aat1* promoter (Fig. 3B). In addition, truncation experiments demonstrated that structural integrity of *CgPOU3F4-like* was essential for activation of *CgB-aat1* promoter. When deletion of POU or HOX domain, the activations significantly decreased (Fig. 3C). Site directed mutagenesis assay was applied to validate three key *CgPOU3F4-like* binding sites (from -632 to -350 region), respectively. The promoter activity was significantly decreased when every site was mutated (Fig. 3D). CHIP-PCR analysis showed that no band was tested in

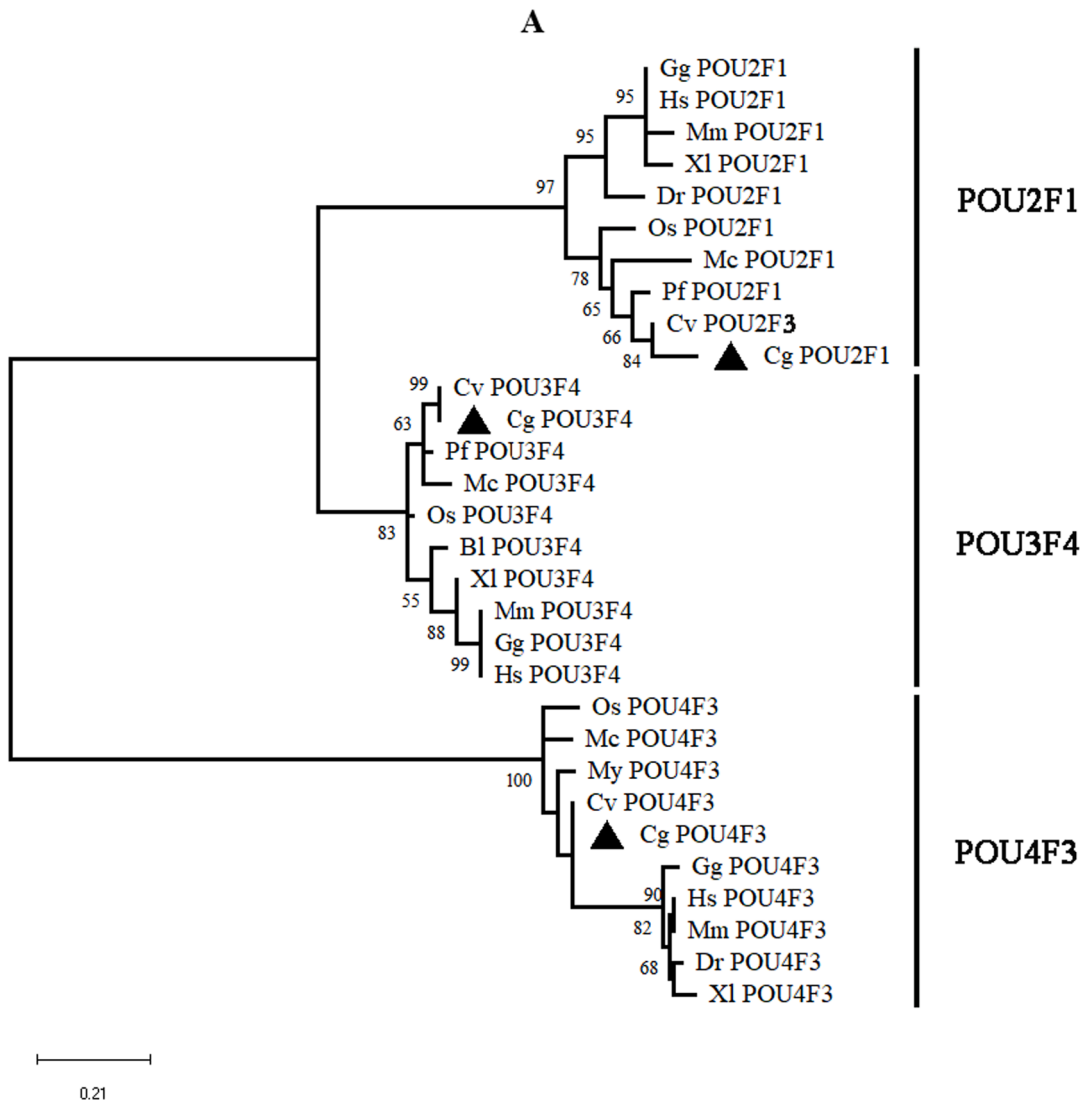
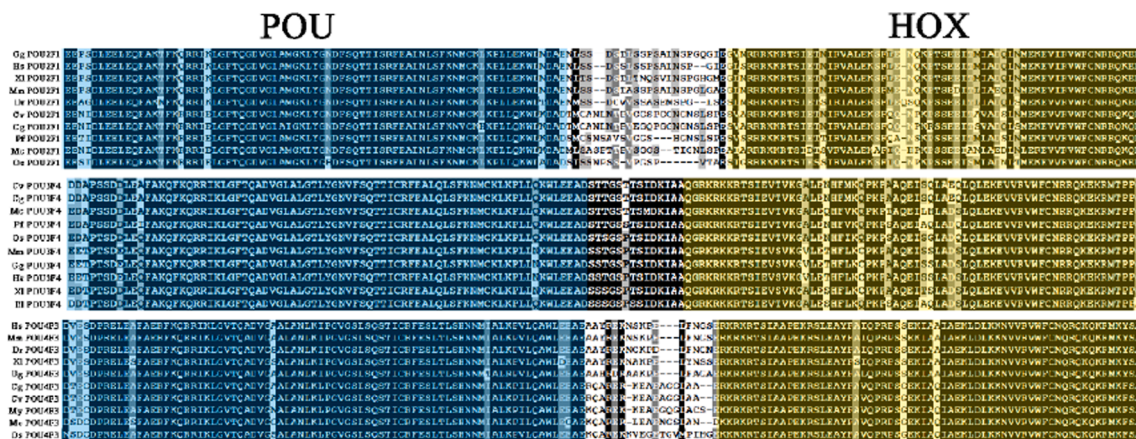


Fig. 1. Multiple sequence alignment and phylogenetic analysis of *POU2F1*, *POU3F4* and *POU4F3*. The partial amino acid sequence was used the followed analysis. (A) Comparison of deduced amino acid sequences of *POU2F1*, *POU3F4* and *POU4F3* among different species. The predicted conserved POU domain (POU₃) and HOX (POU_H) domain among species were highlighted in blue and yellow background, respectively. (B) Phylogenetic tree of three proteins. The tree was generated by the maximum-likelihood algorithm with Jones-Taylor-Thorntton (JTT) + Gamma Distributed (G) model using the MEGA X. The bootstrap values were calculated with 1000 replicates and the numbers at the forks indicated the bootstrap proportions. (For interpretation of the references to color in this figure legend, the reader is referred to the web version of this article.)

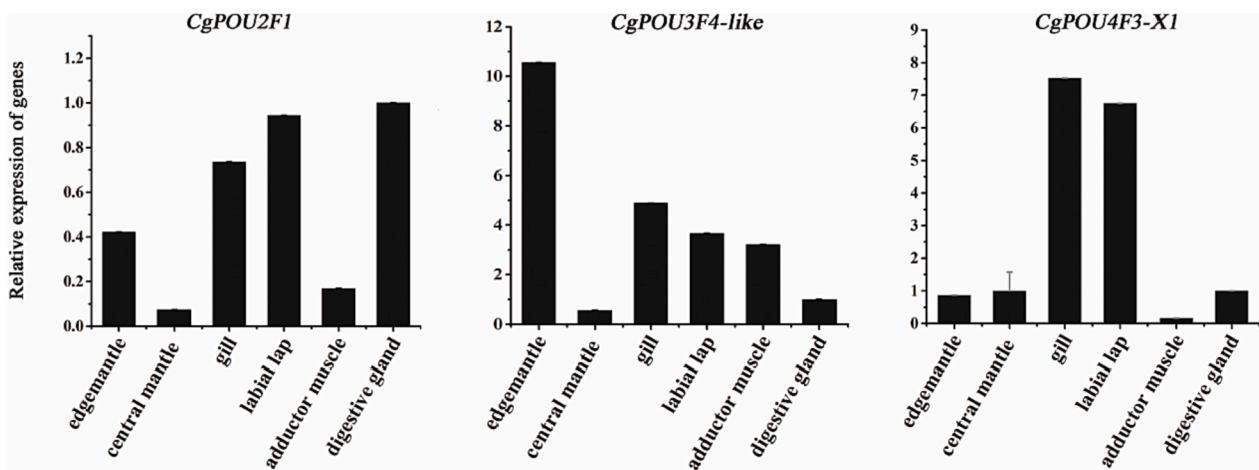


Fig. 2. Expression analysis of *CgPOU2F1*, *CgPOU3F4-like* and *CgPOU4F3-X1* genes in various tissues. There were no significant differences among six tissues of three genes. The digestive gland was used as control. EF1 α was an internal reference gene. All data was shown as mean \pm standard error (SE) (n = 6).

blank or negative group, however, a single band was discovered in Input group or experimental group, respectively (Fig. 4). Taken together, the *CgPOU3F4-like* was able to bind to *CgB-aat1* promoter region and activate *CgB-aat1* gene expression.

3.4. *CgPOU3F4-like* knockdown resulted in decreases of genes and proteins expressions

To confirm whether *CgPOU3F4-like* might regulate *CgB-aat1* gene expression, knocking down *CgPOU3F4-like* *in vivo* using RNAi was carried out. The qPCR results pointed that *CgPOU3F4-like* expression was significantly reduced 93.6% in *CgPOU3F4-like*-RNAi group as compared to the blank group. In addition, the expression levels of *CgB-aat1* and *CgCbs* genes were also significantly decreased by 76% and 89% after *CgPOU3F4-like* silencing, respectively (Fig. 5A). And no matter which gene was expressed, no differences were observed between negative group (EGFP-RNAi) and blank group (nuclease-free water) (Fig. 5A). Additionally, western blot assay showed that *CgPOU3F4-like*, *CgB-aat1* and *CgCbs* proteins were down-regulated by about 50%, 20% and 40% as compared to the blank group, respectively (Fig. 5B). ELISA experiment was employed to analyze the pheomelanin content in mantle after RNAi. Pheomelanin content was slightly reduced in *CgPOU3F4-like* RNAi group, however, there were no obvious differences when compared with control groups (Fig. 5C).

4. Discussion

Although the pivotal role of melanin in shell color formation in oysters have been studied (Feng et al., 2019; Zhu et al., 2021, 2022; Li et al., 2022a), the upstream regulatory mechanisms of transcription factors of shell color-related genes are still poorly understood. In the present study, it was demonstrated that *CgPOU3F4-like* could directly bind to *CgB-aat1* gene promoter and enhance its transcriptional activities, and *CgPOU3F4-like* knockdown led to decreases of expressions of *CgB-aat1* and *CgCbs*, at both mRNA and proteins levels.

Shell color is controlled by different genes related to pigment biosynthesis. Our previous study confirmed that *CgB-aat1* gene was crucial for the regulation of mantle pigments in *C. gigas* (Li et al., 2022c). Here, deduced amino acid sequences of POU family members (*CgPOU2F1*, *CgPOU3F4-like*, *CgPOU4F3-X1*) with POU (POUs) and HOX domains were highly conserved with those sequences from other vertebrates, respectively, suggesting their ability to act as transcription factors in *C. gigas* like in other vertebrates. Additionally, phylogenetic analysis confirmed their identities and constructed their evolution relationships with POU family member from other invertebrates and

vertebrates. The further knowledge of tissue-specific expression patterns of a given gene is valuable for assigning its function. The highest expression of *CgPOU2F1*, *CgPOU3F4-like* and *CgPOU4F3-X1* were observed in digestive gland, mantle edge and gill tissues, respectively, suggesting key roles for *CgPOU2F1* and *CgPOU4F3-X1* in digestion and respiration, and vital role for *CgPOU3F4-like* in shell color formation.

Melanin biosynthesis is a multiple process regulated by a number signaling pathway and transcription factors. In mollusks, the several genes related to melanin synthesis were regulated by several transcription factor, like MITF (Mao et al. 2019; Zhang et al. 2018), paired box gene 3 (PAX3) (Yu et al., 2018b), POU2F1 and SOX5 (Min et al., 2022b). Recent studies reported that transcription factor POU2F1 has been implicated in transcriptional regulation of cystine/glutamate xCT transporter, *Slc7a11* gene (Chen et al., 2019; Yang et al., 2020). However, the transcriptional relationships between three POU members and *CgB-aat1* gene promoters are not clear in bivalves. Co-transfection study demonstrated that only transcriptional factor *CgPOU3F4-like* could bind and have a positive regulatory effect on *CgB-aat1* gene. Site directed mutagenesis assay exploration showed that A/T-rich sites might be high-affinity binding sites for *CgB-aat1*, roughly coinciding with the binding sites for POU_H domain in mammals. This observation was in accordance with result that PPOU3F4 bound to promoter of matrix protein gene in *P. fucata* (Gao et al., 2016), and the DNA binding sites of *CgPOU3F4* also do not contain strictly conserved ATGCAAAT motifs. Because POU domain proteins can recognize diverse DNA sequences based on the structural flexibility of the bipartite POU domain (Andersen et al., 2001), the multitude of roles played by POU domain family members in various processes related to pigmentation in mollusks may be related to the diversity of their binding sites due to their flexible structures. Even so, the mechanism by which *CgPOU3F4* recognizes its binding sites in *CgB-aat1* gene promoters in the Pacific oyster need to be further studied.

Furthermore, RNA interference is a powerful method to inhibit specific gene expression and was used to study the gene function. The transcription factor Pf-Rel, Pf-POU3F4, Pf-C/EBP-A and Pf-C/EBP-B knockdown by RNA interference led to down-regulation of target genes expression, suggesting transcription factor might regulate the expression of target genes (Gao et al., 2016; Chen et al., 2018; Li et al., 2019). Similarly, in the present study, *CgPOU3F4* knockdown led to a significant down-regulation in *CgB-aat1* genes expression, the same true for protein expressions, suggesting that *CgPOU3F4-like* knockdown depressed the transcriptional activity of *CgB-aat1* gene promoter and further effected transcription and translation process of *CgB-aat1* gene. So, this result directly evidenced that *CgB-aat1* expression was regulated by *CgPOU3F4-like*. It was reported that cystine is transported into cell

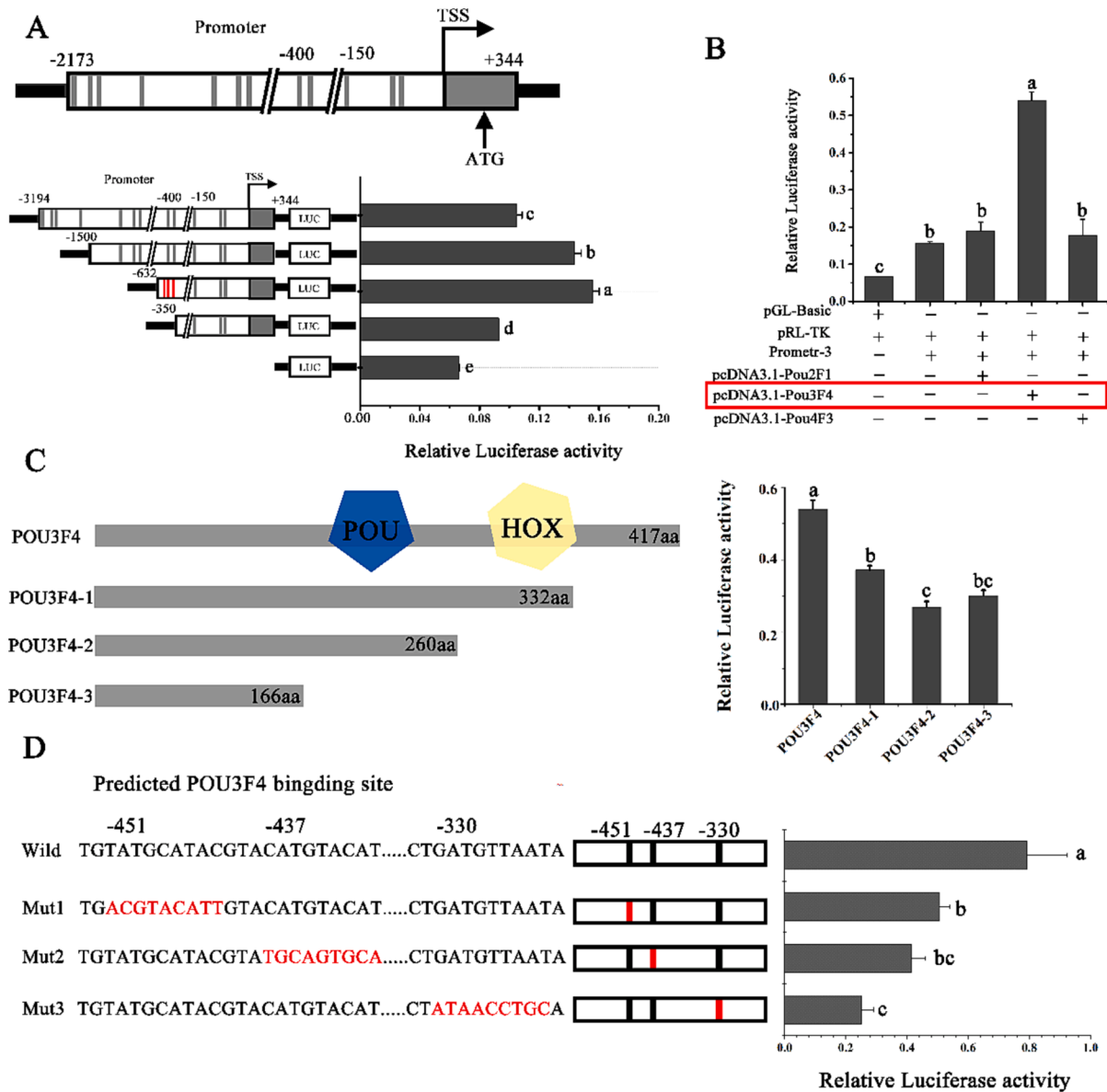


Fig. 3. CgPOU3F4-like regulated the promoter activity of *CgB-aat1* gene. (A) The predicted schematic of *CgB-aat1* gene promoter and the truncation analysis of *CgB-aat1* gene promoter. (B) Enzyme activity measurement of three transcription factor CgPOU2F1, CgPOU3F4-like and CgPOU4F3-X1 on activation of *CgB-aat1* gene promoter. pGL3-basic represents empty carrier group; pRL-TK represents internal control; Prometr-3 represents the core region of promoter group; pcDNA3.1-CgPOU2F1, pcDNA3.1-CgPOU3F4-like and pcDNA3.1-CgPOU4F3-X1 refers to the combined vectors. "+" and "-" means the plasmid was transfected into the HEK-293 T or not. (C) Dual luciferase assay exhibited the effects of truncated CgPOU3F4-like proteins on activation of *CgB-aat1* gene promoter. (D) *CgB-aat1* gene promoter mutation analysis. The wild sequence and mutated site sequence (highlighted in red color) of *CgB-aat1* gene promoter are listed in the left, dual luciferase activity result is shown in the right. Bars represents mean \pm standard deviation (SD) (n = 3). The significant differences ($P < 0.05$) among groups are highlighted by different lowercase letters. (For interpretation of the references to color in this figure legend, the reader is referred to the web version of this article.)

by SLC7a11/xCT, subsequently, cystine and dopaquinone are catalyzed by CBS and consequently promote the pheomelanin synthesis (Barek, 2018; Chintala et al., 2005). In other words, *Cbs* is downstream gene of *B-aat1* in pheomelanin synthesis pathway. In this study, downregulated expression of CgCbs was observed, which was also a proof that CgB-aat1-CgCbs axis was involved in pheomelanin synthesis in *C. gigas*. Intriguingly, pheomelanin content was slightly reduced in CgPOU3F4-like RNAi group, however, there were no dramatic changes among three groups might be due to the short time of interference. These findings uncover that CgPOU3F4-like had a positively regulatory effect on *CgB-aat1* gene expression and it may be a critical upstream transcriptional regulation factor in pheomelanin synthesis.

Colorful shell of bivalves has a direct effect on product value that influences the consumer's behavior at the seafood market. At present,

many different shell colors of bivalves have been produced base on the traditional breeding methods, which has greatly increased the diversity of species (Williams, 2017). However, the relationship between shell color and growth and survival trait was still ambiguity (Han and Li, 2021; Brake et al., 2004; Xu et al., 2017). Recently, high throughput sequencing was used for selecting genes involved in shell coloration (Feng et al., 2015; Hu et al., 2020; Li et al., 2021; Williams et al., 2017; Zhao et al., 2017). Next, the regulatory mechanisms of these selected gene needed to be studied further. This study improves our understanding of the transcriptional regulation shell pigmentation in *C. gigas* at the molecular level and also provides the molecular genetic knowledge of selective breeding of shell coloration lines of bivalves.

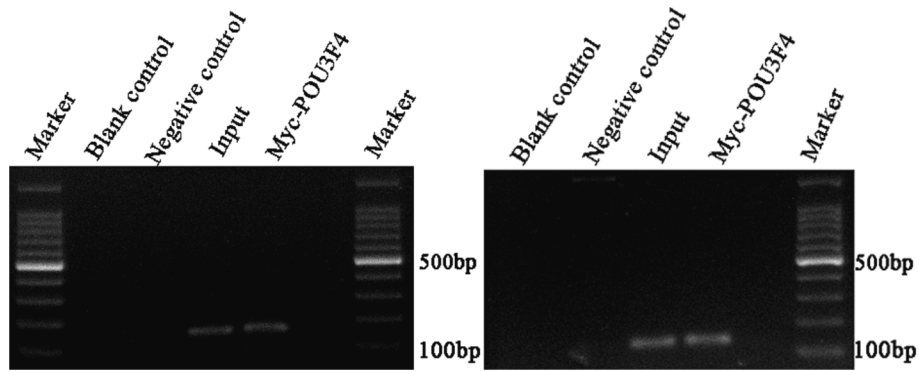


Fig. 4. The binding of CgPOU3F4-like and core regions of CgB-aat1 promoter determined by ChIP. Samples without antibody was used as negative control and without cells was used as blank control. The PCR amplification was applied to detect the binding result base on two pair primers. The first was to detect the former two binding sites (electrophoretic result in left figure), the second was to examine the third binding site (electrophoretic result in right figure).

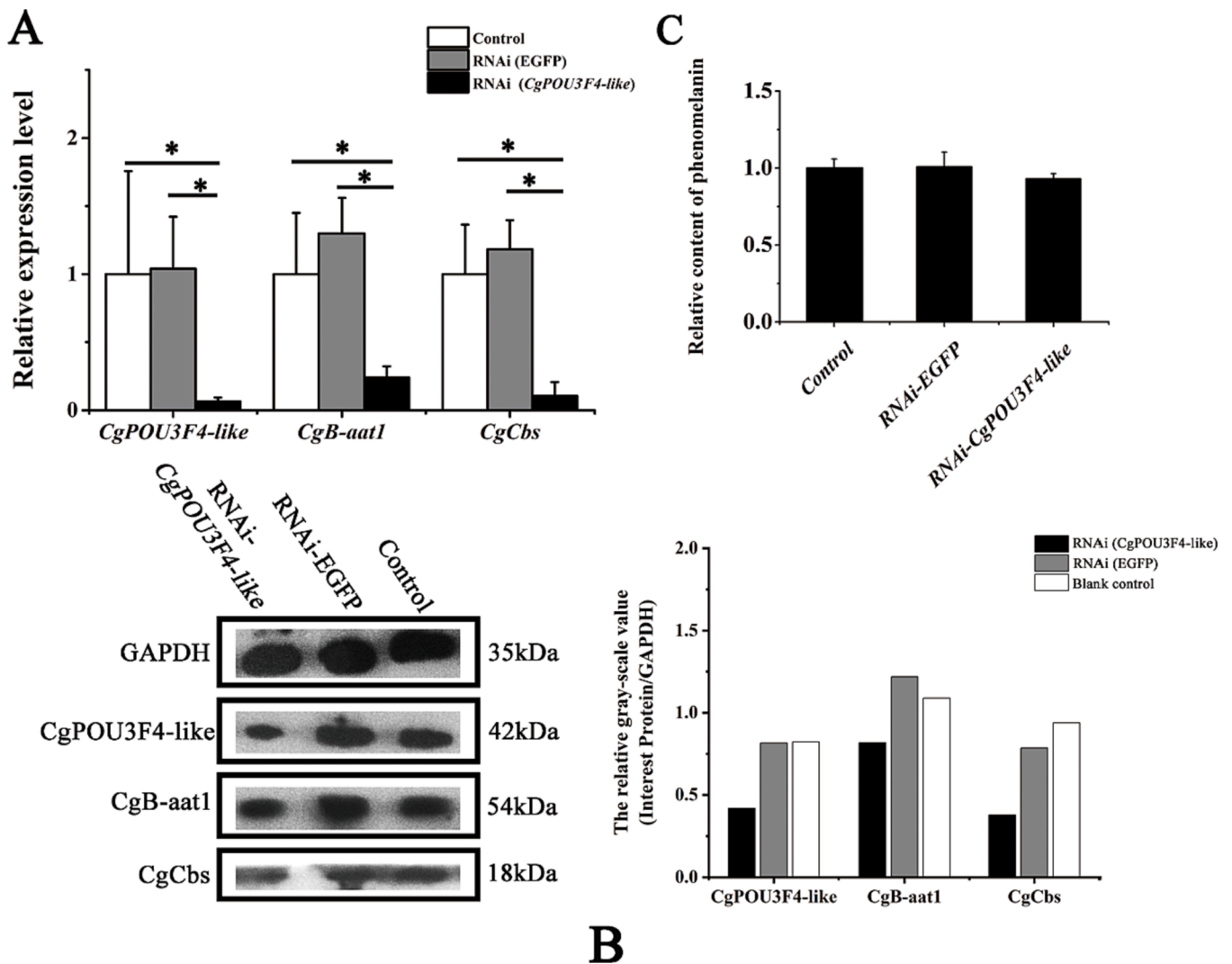


Fig. 5. Expressions of CgPOU3F4-like, CgB-aat1 and CgCbs at mRNA and protein levels as well as pheomelanin content after RNAi. (A) The relative expression levels of CgPOU3F4-like, CgB-aat1 and CgCbs mRNAs in mantle of blank control group, RNAi-EGFP group and RNAi-CgPOU3F4-like group, respectively. The efl α was used as an internal control. All data was shown as mean \pm SE (n = 6). Significant difference was outstanding by * ($P < 0.05$). (B) Proteins expression of CgPOU3F4-like, CgB-aat1 and CgCbs in three groups were analyzed using WB, respectively. Glyceraldehyde-3-phosphate dehydrogenase (GAPDH) was used as internal control. (C) Pheomelanin content in mantle of three groups were detected by Elisa assay.

- Saenko, S.V., Schilthuizen, M., 2021. Evo-devo of shell colour in gastropods and bivalves. *Curr. Opin. Genet. Dev.* 69, 1–5. <https://doi.org/10.1016/j.gde.2020.11.009>.
- Sreenivasan, S., Viljoen, C.D., 2013. OCT1 identity crisis. *Gene* 516, 190–191. <https://doi.org/10.1016/j.gene.2012.12.046>.
- Vu, S.V., Knibb, W., O'Connor, W., Nguyen, N.T.H., In, V.V., Dove, M., Nguyen, N.H., 2020. Genetic parameters for traits affecting consumer preferences for the Portuguese oyster, *Crassostrea angulata*. *Aquaculture* 526, 735391. <https://doi.org/10.1016/j.aquaculture.2020.735391>.
- Wang, J.Q., Hou, L., Yi, N., Zhang, R.F., Zou, X.Y., 2012. Molecular analysis and its expression of a pou homeobox protein gene during development and in response to salinity stress from brine shrimp, *Artemia sinica*. *Comp. Biochem. Physiol. A Mol. Integr. Physiol.* 161 (1), 36–43. <https://doi.org/10.1016/j.cbpa.2011.08.016>.
- Wang, C.D., Liu, B., Liu, X., Ma, B., Zhao, Y.M., Zhao, X., Liu, F.Q., Liu, G.L., 2017. Selection of a new scallop strain, the Bohai Red, from the hybrid between the bay scallop and the Peruvian scallop. *Aquaculture* 479, 250–255.
- Williams, S.T., 2017. Molluscan shell colour. *Biol. Rev.* 92 (2), 1039–1058. <https://doi.org/10.1111/brv.12268>.
- Williams, S.T., Lockyer, A.E., Dyal, P., Nakano, T., Churchill, C.K., Speiser, D.I., 2017. Colorful seashells: identification of haem pathway genes associated with the synthesis of porphyrin shell color in marine snails. *Ecol. Evol.* 7 (23), 10379–10397. <https://doi.org/10.1002/ece3.3552>.
- Wollesen, T., McDougall, C., Degnan, B.M., Wanninger, A., 2014. POU genes are expressed during the formation of individual ganglia of the cephalopod central nervous system. *Evo. Devo.* 5 (41), 1–15. <https://doi.org/10.1186/2041-9139-5-41>.
- Xu, L., Li, Q., Yu, H., Kong, L.F., 2017. Estimates of heritability for growth and shell color traits and their genetic correlations in the black shell strain of Pacific oyster *Crassostrea gigas*. *Mar. Biotechnol.* 19, 421–429. <https://doi.org/10.1007/s10126-017-9772-6>.
- Yang, N.S., Zhao, B.H., Hu, S.S., Bao, Z.Y., Liu, M., Chen, Y., Wu, X.S., 2020. Characterization of POU2F1 gene and its potential impact on the expression of genes involved in fur color formation in rex rabbit. *Genes (Basel)* 11 (5), 575–587. <https://doi.org/10.3390/genes11050575>.
- Yu, F.F., Pan, Z.N., Qu, B.L., Yu, X.Y., Xu, K.H., Deng, Y.W., Liang, F.L., 2018a. Identification of a tyrosinase gene and its functional analysis in melanin synthesis of *Pterea penguin*. *Gene* 656, 1–8. <https://doi.org/10.1016/j.gene.2018.02.060>.
- Yu, F.F., Qu, B.L., Lin, D.D., Deng, Y.W., Huang, R.L., Zhong, Z.M., 2018b. Pax3 gene regulated melanin synthesis by tyrosinase pathway in *Pterea penguin*. *Int. J. Mol. Sci.* 19, 3700. <https://doi.org/10.3390/ijms19123700>.
- Zhang, S.J., Wang, H.X., Yu, J.J., Jiang, F.J., Yue, X., Liu, B.Z., 2018. Identification of a gene encoding microphthalmia-associated transcription factor and its association with shell color in the clam *Meretrix petechialis*. *Comp. Biochem. Physiol. B Biochem. Mol. Biol.* 225, 75–83. <https://doi.org/10.1016/j.cbpb.2018.04.007>.
- Zhang, X.M., Ma, Y.Z., Liu, X.Y., Zhou, Q., Wang, X.J., 2013. Evolutionary and functional analysis of the key pluripotency factor Oct4 and its family proteins. *J. Genet. Genomics* 40 (8), 399–412. <https://doi.org/10.1016/j.jgg.2013.04.011>.
- Zhao, L., Li, Y., Li, Y., Yu, J., Liao, H., Wang, S., Lv, J., Liang, J., Huang, X., Bao, Z., 2017. A genome-wide association study identifies the genomic region associated with shell color in Yesso Scallop, *Patinopecten yessoensis*. *Mar. Biotechnol.* 19, 301–309. <https://doi.org/10.1007/s10126-017-9751-y>.
- Zhu, Y.J., Li, Q., Yu, H., Liu, S.K., Han, Z.Q., Kong, L.F., 2021. Shell biosynthesis and pigmentation as revealed by the expression of tyrosinase and tyrosinase-like protein genes in Pacific oyster (*Crassostrea gigas*) with different shell colors. *Mar. Biotechnol.* 23, 777–789. <https://doi.org/10.1007/s10126-021-10063-2>.
- Zhu, Y.J., Li, Q., Yu, H., Liu, S.K., Kong, L.F., 2022. Expression of tyrosinase-like protein genes and their functional analysis in melanin synthesis of Pacific oyster (*Crassostrea gigas*). *Gene* 840, 146742. <https://doi.org/10.1016/j.gene.2022.146742>.